Front. Struct. Civ. Eng. 2022, 16(2): 175–190
https://doi.org/10.1007/s11709-021-0791-z

RESEARCH ARTICLE

Sensitivity analysis of the deterioration of concrete strength in marine environment to multiple corrosive ions

Jinwei YAO[a,b], Jiankang CHEN[b*]

[a] *Zhejiang Business Technology Institute, Ningbo 315012, China*
[b] *Key Laboratory of Impact and Safety Engineering, Ministry of Education, School of Mechanical Engineering and Mechanics, Ningbo University, Ningbo 315211, China*
[*] *Corresponding author. E-mail: chenjiankang1957@163.com*

ABSTRACT The corrosion degradation behavior of concrete materials plays a crucial role in the change of its mechanical properties under multi-ion interaction in the marine environment. In this study, the variation in the macro-physical and mechanical properties of concrete with corrosion time is investigated, and the source of micro-corrosion products under different salt solutions in seawater are analyzed. Regardless of the continuous hydration effect of concrete, the damage effects of various corrosive ions (Cl^-, SO_4^{2-}, and Mg^{2+}, etc.) on the tensile and compressive strength of concrete are discussed based on measurement in different salt solutions. The sensitivity analysis method for concrete strength is used to quantitatively analyze the sensitivity of concrete strength to the effects of each ion in a multi-salt solution without considering the influence of continued hydration. The quantitative results indicate that the addition of Cl^- can weaken the corrosion effect of SO_4^{2-} by about 20%, while the addition of Mg^{2+} or Mg^{2+} and Cl^- can strengthen it by 10%–20% during a 600-d corrosion process.

KEYWORDS sensitivity analysis, concrete strength, corrosion deterioration, multi-ion interaction, marine environment

1 Introduction

The corrosion damage of concrete structures in marine environments has always been a hot research issue [1–6]. Such marine structures are regularly exposed to abundant corrosive sea salts, which causes severe corrosion damage much earlier than the end of their theoretically designed service life. Sea water primarily contains salts such as NaCl, $MgCl_2$, KCl, and $MgSO_4$, and the ion content of Cl^-, Mg^{2+}, and SO_4^{2-} is high in these salt solutions. For example, the concentrations of Cl^-, Mg^{2+}, and SO_4^{2-} in the sea water near Shanghai Yangshan Port in the East China Sea are 14642, 918, and 592 mg/L, respectively. Although studies have shown that Cl^- mainly causes corrosion of steel bars in reinforced concrete, Mg^{2+} and SO_4^{2-} mainly corrode concrete cement-based materials, but Cl^- still corrodes the cement matrix, causing damage to the concrete itself [7,8]. Moreover, the interaction of these three harmful ions in seawater causes greater corrosion damage to the structure than that caused by a single ion species [9]. Therefore, the corrosion of concrete materials in marine environment cannot be explained by only considering a single ion, and it is necessary to clarify the degradation mechanism and degree of corrosion damage in the case of multi-ion interaction.

Usually, a compound solution of chloride and sulfate is used to simulate seawater corrosion solution, and there are many reports on the corrosion damage of cement-based materials based on this [10–13]. In the corrosion process, the destructive effect of the two harmful ions (Cl^- and SO_4^{2-}) due to the cross-competition between them is significantly different from that of a single ion. The main conclusions are divided into two parts: 1) The corrosion effect of SO_4^{2-} on concrete materials in the presence of chloride salt. Since Cl^- in the chloride salt diffuses faster than SO_4^{2-} (the former is 10–100 times

Article history: Received Aug 7, 2021; Accepted Oct 18, 2021

faster than the latter), it can enter the concrete material before SO_4^{2-} and chemically react with hydration products to form Friedel's Salt, which fills up the internal pores and temporarily delays the intrusion of SO_4^{2-} into the material; 2) The corrosion effect of Cl^- on concrete materials in the presence of sulfate. Sulfate can reduce the amount of Cl^- bound to the hydration products and increase the concentration of free Cl^- in the solution. Because SO_4^{2-} can not only decompose Friedel's salt, but also react with tricalcium aluminate in the unhydrated cement or AFm of the hydrated product first to inhibit the formation of Friedel's salt [14].

In addition, the numerical simulation method is an effective research method to study the impact of multi-ionic affected concrete in the marine environment and subject to various degradation processes [15]. Compared with experimental research methods, this method has greater advantages in studying combination effects and providing more visual information [16]. There are numerical models that can be used to describe the chloride diffusion process under complex environments and clarify the mechanisms between them [17–19]. There are many numerical models for the numerical evaluation of external sulfate attack on the concrete structures [20]. There are also numerical studies on external sulfate attack and its influence on the bonding and diffusion of chloride in concrete [21,22].

In the compound solution of chloride and sulfate, most researchers often focus on only the destructive effects of anions (Cl^- and SO_4^{2-}) but ignore the effects of different cations (especially Mg^{2+}) on the corrosion damage of materials. In fact, magnesium ions in the mixed corrosion solution play a crucial role in the corrosion degradation of concrete [23–26]. Once the Mg^{2+} ions in the solution enter the concrete pores, the amount of $Ca(OH)_2$ in the internal solution is reduced, which in turn causes the pH value in the pore solution to drop. This finally leads to decalcification of C−S−H gel and converts it into M−S−H. Since M−S−H has no adhesiveness, the concrete structure becomes loose and its strength is greatly reduced [27]. Maes et al. [28] showed that the effect of sodium sulfate and magnesium sulfate on the penetration of chlorides in concrete or mortar is closely related to the cations(especiallyMg^{2+}).Itisincorrecttogeneralizetheinfluence of sulfate attack on the diffusion mechanism of Cl^-, and the actual content of Mg^{2+} in seawater is generally higher than that of SO_4^{2-}. Therefore, the influence of Mg^{2+} must be considered when using the compound solution of chloride and sulfate to simulate seawater corrosion. Consequently, to simulate the actual marine environment and accurately predict the durability of concrete materials, it is imperative to use multi-ion (Cl^-, SO_4^{2-}, and Mg^{2+}) corrosion solutions to examine the corrosion damage of these materials.

In fact, the change in the macro-mechanical properties of materials is the most direct reflection of the degree of corrosion damage, and the strength indicators of the material (such as compressive strength, tensile strength, etc.) are some of the other direct parameters for evaluating corrosion damage. Although there are several reports on the strength degradation of concrete materials by the composite solution of Cl^- and SO_4^{2-} [29–31], the corrosive effect of the composite solution of multiple ions (Cl^-, Mg^{2+}, and SO_4^{2-}) on the macro-mechanical properties of concrete has been rarely investigated, and the evolution of corrosion damage has not yet been clarified yet. By studying the macro-physical properties of the material (such as mass loss and dynamic elastic modulus change as indicators), Yu et al. [32] found that the corrosion effect of the mixed solution of Cl^-, SO_4^{2-}, and Mg^{2+} on concrete materials was significantly more serious than that of the mixed solution of SO_4^{2-} and Mg^{2+}. The addition of Cl^- could not alleviate the chemical corrosion caused by SO_4^{2-} and Mg^{2+}, but it accelerated the chemical corrosion damage. However, this conclusion is different from the results of Maes and de Belie [33]. This may be attributed to the different composition of the corrosion solution and the length of the corrosion period. Furthermore, the micro-corrosion mechanism of concrete by the multi-ion (Cl^-, Mg^{2+}, and SO_4^{2-}) composite solution is not fully understood, and the corrosion mechanism of the three interactive competitions is extremely complicated [34–36].

In this study, the corrosion of concrete with different water-cement ratios in different seawater salt solutions is experimentally investigated. By testing the compressive strength and splitting tensile strength of concrete at different corrosion times, the influence of different seawater corrosion solutions on the mechanical properties of concrete is analyzed. The effect of different corrosion solutions on the damage of concrete shape is examined by comparing by change in the appearance of concrete at different corrosion times. Further, by measuring the changes in the microscopic composition of the concrete specimens, the influence of different corrosion solutions on the microscopic damage of the concrete sample is studied. Using a combination of macro and micro methods, the effect of various corrosion ions in different salt solutions on the concrete corrosion damage is examined, and a sensitivity analysis index based on the strength factor of concrete is established. Furthermore, quantitative sensitivity analysis is conducted to analyze the corrosion of concrete induced by the interaction of magnesium-sulfate-chloride ions.

2 Materials and methods

2.1 Material preparation

1) Cement: Ordinary Portland cement was used for the

experiment. The cement strength grade was 42.5 MPa. X-ray fluorescence spectroscopy was used to analyze the chemical composition of cement, and the results are shown in Table 1. The particle size of cement powder was evaluated by a laser particle size analyzer, and the results are listed in Fig. 1.

2) Fine aggregate: ISO standard sand was used. The particle distribution is shown in Table 2.

3) Coarse aggregate: The coarse aggregate used to make concrete was 5–16 mm continuous gradation of gravel. Its particle gradation is shown in Table 3.

4) Water: Distilled water was used for the preparation of concrete specimens, and the local tap water from Ningbo, China was used to prepare the soaking solution.

2.2 Proportioning design and sample production

The designed mix ratios, by mass, of concrete are presented in Table 4. A total of two mix ratios are considered, with water-cement ratios of 0.50 and 0.33. ABS engineering plastic test molds were used to make concrete specimens for examining tensile and compressive strength. The concrete specimen for compressive strength test is a cube with a size of 100 mm × 100 mm ×100 mm, and that for splitting tensile strength test is a cylinder with a diameter of 100 mm and thickness of 50 mm.

The concrete specimens were demolded after they were cured at a room temperature for 24 h. Subsequently, they were cured in clean water in the laboratory for 28 d and then were put into various solutions for complete immersion corrosion tests. The corrosion solution was divided into 6 kinds of solutions according to their composition: clear water solution (represented by the symbol "Q"), NaCl solution with a mass fraction of 10% (represented by the symbol "L"), Na_2SO_4 solution with a mass fraction of 5% (represented by the symbol "S"), $MgSO_4$ solution with a mass fraction of 5% (represented by the symbol "M"), mixed solution of 5% Na_2SO_4 and 10% NaCl (represented by the symbol "SL"), and mixed solution of 5% $MgSO_4$ and 10% NaCl (represented by the symbol "ML"). The composition of designed solutions is shown in Table 5.

2.3 Test method

The entire corrosion experiment lasted for 600 d. The concrete specimens were removed from the corrosion solution, and their strength was tested on the 0th, 30th, 90th, 180th, 270th, 360th, 450th, and 600th day (see Fig. 2). Three specimens were used for each compression and splitting tensile test. In the compressive strength test, the displacement loading rate was 0.6 mm/min, and the corresponding strain rate was 1×10^{-4}. Further, in the splitting tensile strength test, a displacement loading rate of 0.06 mm/min was used, i.e., the strain rate was 1×10^{-5}. ASTM C 496 splitting tensile test method was used to test

Table 1 Chemical composition of cement (wt.%)

Al_2O_3	CaO	Fe_2O_3	K_2O	MgO	Na_2O	SO_3	SiO_2	TiO_2	loss
5.55	67.18	4.19	0.91	1.71	0.32	3.18	15.92	0.59	0.45

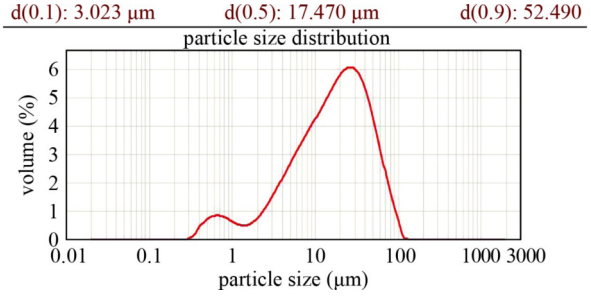

Fig. 1 Particle size distribution of cement particles.

Table 2 Particle distribution of reference sand

side length of square hole (mm)	cumulative sieve residue (%)
0.08	99 ± 1
0.16	87 ± 5
0.50	67 ± 5
1.00	33 ± 5
1.60	7 ± 5
2.00	0

Table 3 Particle size distribution of gravel

side length of square hole (mm)	sieve weight (g)	cumulative weight percentage (%)	5–16 mm continuous gradation cumulative sieve residue (%)
2.36	45.3	97.00	95–100
4.75	460.5	92.47	85–100
9.50	425.7	46.42	30–60
16.0	38.5	3.85	0–10
19.0	0	0	0

Table 4 Mix design of concrete (wt.%)

type	water-cement ratio (*w/c*)	cement	water	sand	gravel
I	0.33	22	7	21	50
II	0.50	14	7	29	50

Table 5 Design of concentration of corrosive solution (wt.%)

symbol	NaCl	Na_2SO_4	$MgSO_4$	water
Q	0	0	0	100
L	10	0	0	90
S	0	5	0	95
M	0	0	5	95
SL	10	5	0	85
ML	10	0	5	85

the splitting tensile strength of concrete. The strength of concrete specimens was calculated by using the following equation:

$$T = \frac{2P}{\pi ld}, \tag{1}$$

where T is the splitting tensile strength, P is the failure load, l is the length of the specimen, and d is the diameter of the specimen.

During the entire corrosion experiment, the appearance and morphology of the concrete specimens, especially the changes on the outer surface of concrete (surface cracks, corners, surface peeling, etc.), were analyzed by making images. The microscopic damage mechanism of concrete material was analyzed, and the variation in material composition of the cement paste sample was detected by X-ray diffraction (XRD) after 1, 4, 10, and 12 months. Scanning electron microscopy (SEM) was used to examine the microscopic morphology and elemental composition of the concrete samples.

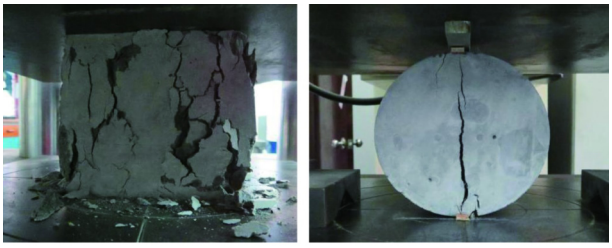

Fig. 2 Concrete failure state: (a) compressive failure; (b) tensile failure.

3 Results and discussion

3.1 Variation trend of the compressive and tensile strengths of concrete in different corrosive solutions

The variation in the compressive and tensile strengths of concrete as a function of corrosion time under different water-cement ratios in the six corrosion solutions is shown in Fig. 3. Here, the symbols "f" and "y" represent the compressive strength and tensile strength, respectively. The symbols "q5" and "q3" stand for the strength values of concrete soaked in clean water with water-cement ratios of 0.50 and 0.33, respectively, where the letter "q" represents a clear aqueous solution (Q). Simi-

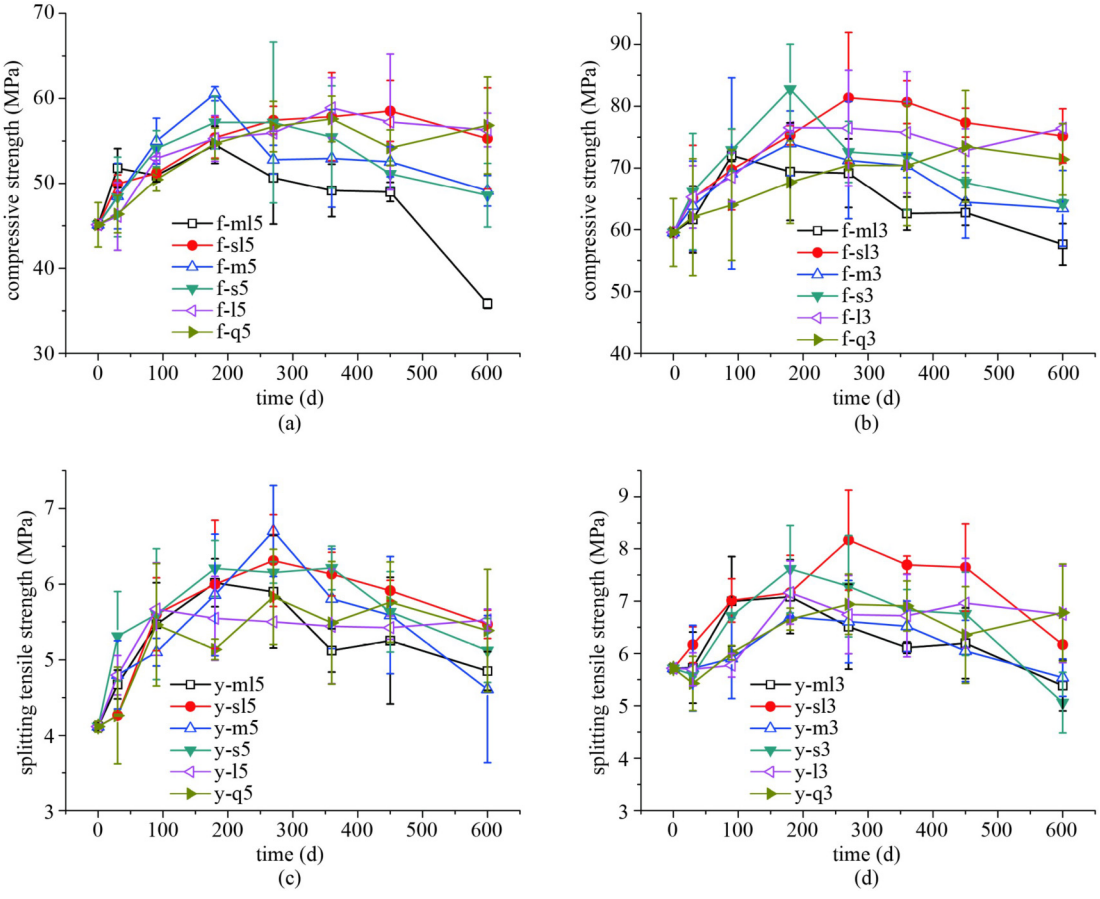

Fig. 3 Relationship between concrete strength and corrosion time. (a) w/c = 0.50, compressive strength; (b) w/c = 0.33, compressive strength; (c) w/c = 0.50, tensile strength; (d) w/c = 0.33, tensile strength.

larly, l5 and l3 denote the strength values of concrete in sodium chloride solution (L); s5 and s3 are the strength values of concrete in pure sodium sulfate solution (S); m5 and m3 are the strength values of concrete samples immersed in magnesium sulfate solution (M); sl5 and sl3 are the strength values of concrete in composite solution of sodium sulfate and sodium chloride (SL); ml5 and ml3 are the strength values of concrete in the composite solution of magnesium sulfate and sodium chloride (ML).

It is clear from Fig. 3 that the tensile and compressive strengths of concrete with a large water-cement ratio are smaller than those of concrete with a small water-cement ratio. During the entire immersion process in the six kinds of solutions, the maximum and minimum compressive strengths of concrete specimens with water-cement ratios of 0.50 are 60.6 and 35.8 MPa, respectively; the maximum and minimum tensile strengths are 6.7 and 4.1 MPa, respectively. For concrete specimens with a water-cement ratio of 0.33, the maximum and minimum compressive strengths are 82.8 and 57.6 MPa, respectively; the maximum and minimum tensile strengths are 8.2 and 5.1 MPa, respectively.

The above strength curves are normalized with respect to the initial strength value of concrete in Fig. 4. It is evident that the strength of concrete specimens with different water-cement ratios increases during the early stage of soaking (approximately 0 to 200 d). However, the increase in the strength of concrete in clear aqueous solution is lower than that in other solutions. This indicates that in addition to the continued enhancement of the hydration reaction, the concrete strength is enhanced by the reaction products of the ions in the salt solution with the concrete material itself. During the late stage of corrosion (after soaking for approximately 200–300 d), the strength values of concrete in the four solutions (ML, SL, M, and S) show a decreasing trend. In terms of compressive strength, the specimens in the ML solution show the largest decrease, and those in Q and L solutions exhibit the smallest or no decrease. It is noteworthy that the addition of sodium chloride in the sodium sulfate solution and the magnesium sulfate solution has different effects on the corrosion damage of the concrete materials. Compared with the compressive strength, except for the concrete specimens in Q and L solutions in which there is basically no downward trend, the specimens in the other solutions have a more obvious downward trend of tensile strength.

Especially in Fig. 4(a), the compressive strength of

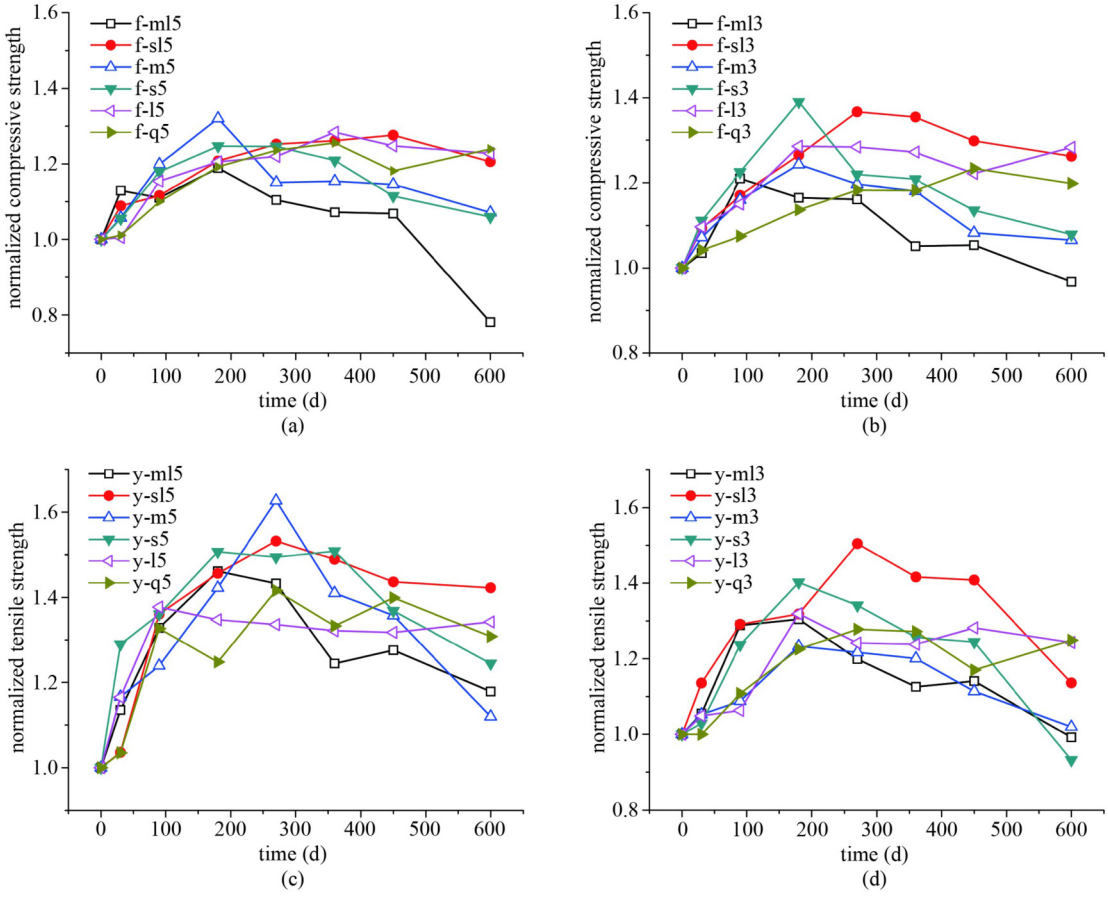

Fig. 4 Relationship between normalized strength and corrosion time. (a) w/c = 0.50, normalized compressive strength; (b) w/c = 0.33, normalized compressive strength; (c) w/c = 0.50, normalized tensile strength; (d) w/c = 0.33, normalized tensile strength.

f-ml5 is significantly lower than that of others. The main reason is that once the magnesium ions in the corrosive solution enter the concrete pores, they will produce incompatible magnesium hydroxide, reduce the fall in pH in the pore solution, promote the decalcification of C−S−H gel and convert it into M−S−H. As a result, the concrete structure becomes loose and its strength is greatly reduced [27]. In addition, compared with that of a water-cement ratio of 0.33, the internal porosity of the concrete material with a water-cement ratio of 0.5 is larger, the corrosion ion diffusion rate is faster, and it is more likely to cause damage. Therefore, the compressive strength of f-ml5 decreases significantly by the 600th day.

3.2 Sensitivity analysis based on strength factor

Through the experimental test, the variation curve of concrete strength in different solutions with corrosion time is obtained. Figure 4 shows that the ML solution causes a greater degree of damage and degradation to the compressive strength of concrete than other solutions, but the degree of corrosion of the concrete caused by each ion cannot be determined quantitatively. Here, a sensitivity factor is introduced to quantify the contribution of continuous hydration and corrosive ions to the concrete strength as well as to analyze the influence of the interaction of each ion in the corrosion solution on the concrete strength.

The initial value of concrete strength is defined as σ_0, and σ_Q, σ_L, σ_S, σ_M, σ_{SL}, and σ_{ML}. These represent the strength value of concrete immersed in clear water (Q), sodium chloride solution (L), sodium sulfate solution (S), magnesium sulfate solution (M), sodium chloride and sodium sulfate composite solution (SL), and sodium chloride and magnesium sulfate composite solution (ML) on the tth day. In different solutions, the influence coefficients are represented by the symbols $\eta_Q(t)$, $\eta_L(t)$, $\eta_S(t)$, $\eta_M(t)$, $\eta_{SL}(t)$, and $\eta_{ML}(t)$, respectively, which indicate the ratio of the strength on the tth day to its initial strength, i.e., $\sigma_Q = \sigma_0\eta_Q(t)$.

In the corrosive solution, the combined effect of corrosive ions and continuous hydration affects the strength of the material, while in the clear aqueous solution, only the continuous hydration reaction affect the strength. Therefore, the strength of concrete in the clear water solution is used as a control, and the value of the strength of the material in the corrosive solution divided by the strength in the clear water solution is used as the sensitivity factor.

Now, the sensitivity factor λ is introduced, where $\lambda(t)$ is defined as the ratio of the influence coefficient $\eta(t)$ of the concrete immersed in two different solutions on the tth day, i.e., $\lambda_{L/Q}(t) = \eta_L(t)/\eta_Q(t)$. When $\lambda_{L/Q}(t) < 1$ (or $\lambda_{L/Q}(t) > 1$), it implies that the addition of Cl^- to the clear water solution weakens (or strengthens) the increase in strength. When $\lambda_{L/Q}(t) = 1$, it indicates that Cl^- has no effect on the change in concrete strength.

In this article, the experimental data has a form of enhancement or reduction, and this property can be better fitted with a quadratic polynomial. Therefore, a quadratic polynomial is used to fit the normalized intensity value vs. corrosion time curves in Fig. 4, and the fitting parameters are shown in Tables 6–9. The polynomial is as follows:

$$\eta(t/t_0) = B_2(t/t_0)^2 + B_1(t/t_0) + 1, \quad (2)$$

where η is the normalized strength value of each concrete specimen, t indicates the corrosion time, t_0 is defined as 1 d, and B_1 and B_2 are undetermined coefficients.

To analyze the influence of various ions in seawater on the evolution of concrete strength, the increase in strength caused by the continued hydration is not calculated, and the sensitivity analysis of the strengthening or weakening effect of each ion in the solution on the change in concrete strength, only, is considered. According to the experimental results in Fig. 4, Eq. (2) is used to fit the data in Fig. 4 to obtain a fitting curve. Then, the curve obtained by fitting each corrosion solution divided by the fitting curve in the clear water solution is defined as the sensitivity factor in Fig. 5. During the process of immersion in corrosion solution, except for the minor effect of sodium chloride solution on the tensile strength value, the effects of the ions on the increase in the tensile and compressive strength of concrete show a general trend of strengthening ($\lambda > 1$) first and then weakening ($\lambda < 1$). The effect of each ion on the tensile strength of concrete is greater than that on the compressive strength, and for the concrete sample with a small compressive strength and water-cement ratio, the strengthening effect of each ion on the increase in concrete strength is longer. However, the transition point between strengthening and weakening effect is quite different for different specimens, which is closely related to the water-cement ratio of the test piece and the ions in the corrosion solution, as shown in Tables 10 and 11. Generally, the

Table 6 Parameter fitting results of compressive strength of concrete with $w/c = 0.50$

η_c	normalized strength value					
	5% $MgSO_4$ + 10% NaCl	5% Na_2SO_4 + 10% NaCl	5% $MgSO_4$	5% Na_2SO_4	10% NaCl	water
B_2	-2.821×10^{-6}	-1.836×10^{-6}	-2.356×10^{-6}	-2.588×10^{-6}	-1.649×10^{-6}	-1.360×10^{-6}
B_1	1.331×10^{-3}	1.436×10^{-3}	1.460×10^{-3}	1.581×10^{-3}	1.3348×10^{-3}	1.167×10^{-3}
R^2	0.862	0.968	0.788	0.989	0.952	0.938

Table 7 Parameter fitting results of compressive strength of concrete with $w/c = 0.33$

η_c	normalized strength value					
	5% $MgSO_4$ + 10% NaCl	5% Na_2SO_4 + 10% NaCl	5% $MgSO_4$	5% Na_2SO_4	10% NaCl	water
B_2	-2.054×10^{-6}	-2.560×10^{-6}	-2.234×10^{-6}	-3.066×10^{-6}	-1.901×10^{-6}	-0.981×10^{-6}
B_1	1.113×10^{-3}	1.932×10^{-3}	1.370×10^{-3}	1.862×10^{-3}	1.532×10^{-3}	0.925×10^{-3}
R^2	0.848	0.977	0.974	0.887	0.971	0.978

Table 8 Parameter fitting results of tensile strength of concrete with $w/c = 0.50$

η_t	normalized strength value					
	5% $MgSO_4$ + 10% NaCl	5% Na_2SO_4 + 10% NaCl	5% $MgSO_4$	5% Na_2SO_4	10% NaCl	water
B_2	-4.041×10^{-6}	-3.869×10^{-6}	-5.254×10^{-6}	-5.083×10^{-6}	-2.794×10^{-6}	-2.764×10^{-6}
B_1	2.590×10^{-3}	2.922×10^{-3}	3.286×10^{-3}	3.340×10^{-3}	2.130×10^{-3}	2.136×10^{-3}
R^2	0.937	0.965	0.911	0.658	0.846	0.840

Table 9 Parameter fitting results of tensile strength of concrete with $w/c = 0.33$

η_t	normalized strength value					
	5% $MgSO_4$ + 10% NaCl	5% Na_2SO_4 + 10% NaCl	5% $MgSO_4$	5% Na_2SO_4	10% NaCl	water
B_2	-3.017×10^{-6}	-4.482×10^{-6}	-2.400×10^{-6}	-4.486×10^{-6}	-1.778×10^{-6}	-1.628×10^{-6}
B_1	1.719×10^{-3}	2.905×10^{-3}	1.435×10^{-3}	2.546×10^{-3}	1.443×10^{-3}	1.324×10^{-3}
R^2	0.833	0.933	0.973	0.938	0.836	0.891

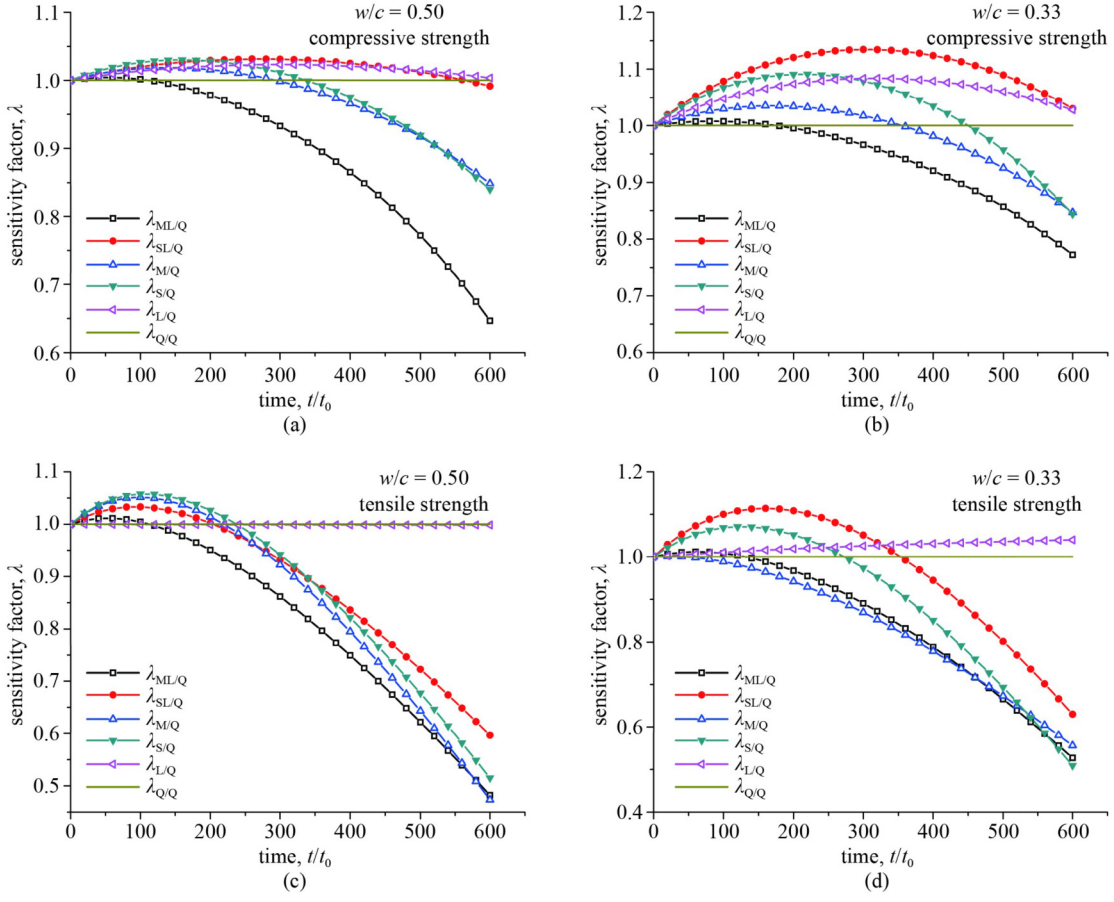

Fig. 5 Sensitivity analysis of each ions to the strength of concrete. (a) $w/c = 0.50$, sensitivity analysis of compressive strength; (b) $w/c = 0.33$, sensitivity analysis of compressive strength; (c) $w/c = 0.50$, sensitivity analysis of tensile strength; (d) $w/c = 0.33$, sensitivity analysis of tensile strength.

Table 10 The transition time point between strengthening and weakening of compressive strength

w/*c*	ML	SL	M	S	L
0.50	110	560	290	335	600
0.33	175	>600	355	450	>600

Table 11 The transition time point between strengthening and weakening of tensile strength

w/*c*	ML	SL	M	S	L
0.50	110	205	220	235	–
0.33	130	350	45	270	–

smaller the water-cement ratio, the lower the porosity, the greater the impact of ions on the concrete strength value, and the greater the sensitivity.

During the strengthening stage, ML solution hardly increases the compressive strength of concrete with w/c = 0.50, and the others increase the strength by approximately 3%–5%. For concrete with w/c = 0.33 also, ML solution hardly increases the strength, but M solution increases it by approximately 4%, both S and L solutions increase it by approximately 9%, and SL solution increases it by approximately 13%. Similar to the compressive strength of concrete, ML solution causes almost no change in the tensile strength of concrete with w/c = 0.50 and w/c = 0.33. Regarding the influence of other harmful ions on the change in tensile strength of concrete with w/c = 0.50, M, S, and SL solutions increase the strength by approximately 5%, 6%, and 4%, respectively, while the L solution does not affect it. Further, for concrete with w/c = 0.33, M solution does not affect tensile strength, while S and SL solutions increase it by approximately 8% and 13%, respectively, and L solution causes a continuous increase in the tensile strength, but the increase is small.

At 600 d of corrosion, due to the influence of harmful ions found in seawater solution on the compressive strength of concrete with w/c = 0.50, ML solution reduces the strength value by approximately 35%, and both M and S solutions reduce it by approximately 15%. The SL and L solutions have almost no effect on the strength. Further, for concrete with w/c = 0.33, ML solution decreases the strength by approximately 23%, and both M and S solutions decrease it by approximately 15%, but the SL and L solutions increase it by 3%. In terms of the influence of the harmful ions on the tensile strength, except for the L solution which does not affect or slightly strengthens it, the tensile strengths of the concrete samples with the two water–cement ratios in the other corrosive solutions are reduced by approximately 40%–50%.

It was generally believed that sodium chloride solution had a minor effect on the deterioration of concrete strength. However, our results indicated that sodium chloride solution had a significant effect, especially on the compressive strength. In comparison to the compressive strength, the effect on the tensile strength was less.

In general, during the entire corrosion process, the degree of effect of the corrosion solutions on the strength degradation performance was in the following order: ML > M > S > SL > L. When the corrosion reaches 600 d, the deterioration of tensile strength of the concrete material was greater than that of the compressive strength, which means that the corrosion solution has a stronger impact on the tensile strength than the compressive strength.

Although SO_4^{2-} in the sulfate solution plays a major role in the deterioration of concrete strength, the addition of Cl^- and Mg^{2+} in the corrosive solution affects SO_4^{2-}, which can delay or accelerate the deterioration. To investigate the influence of the interaction between various ions in the sulfate solution on the evolution of concrete strength, the sensitivity of the interaction between Cl^-, Mg^{2+}, and SO_4^{2-} ions to strengthen or weaken the change in concrete strength is analyzed, as shown in Fig. 6. It is clear from the figure that although SO_4^{2-} in the solution corrodes the concrete material, the addition of only Cl^- delays the deterioration of the strength by SO_4^{2-}. For example, when the corrosion reaches 600 d, the strength of concrete in the SL solution is approximately 20% higher than that in the S solution. The addition of Mg^{2+} or both Cl^- and Mg^{2+} in sulfate solution accelerates the degradation effect of SO_4^{2-} by 10%–20% on the concrete strength, and the corrosion degradation effect of ML solution is generally stronger than that of M solution. However, during the later stage of corrosion, especially after 550 d and until 600 d, these ions may delay the increase in the strength value. That is, the addition of these ions may reduce the corrosion degradation effect of SO_4^{2-}. For example, at 600 d of corrosion, the compressive strength of concrete in M solution is almost equal to that in S solution.

Overall, through the quantitative sensitivity analysis, it can be inferred that the addition of Cl^- ions, only, in the sulfate solution delays the deterioration of concrete strength to a certain extent, while the addition of Mg^{2+} or Cl^-, Mg^{2+} ions accelerates it during the early stage of corrosion. However, these corrosive ions may delay the strength degradation during the later stage.

3.3 Surface appearance in different corrosive solutions

After 600 d of immersion in various corrosion solutions, the images of the concrete surfaces are obtained, as shown in Figs. 7 and 8. It is evident that the surface peeling and edge peeling in ML and M solutions are more serious, and the edge peeling of ML5 and ML3 specimens is more severe than that of M5 and M3 specimens, while the surface peeling of M5 and M3 specimens is higher. When the concrete specimens are soaked in ML and M

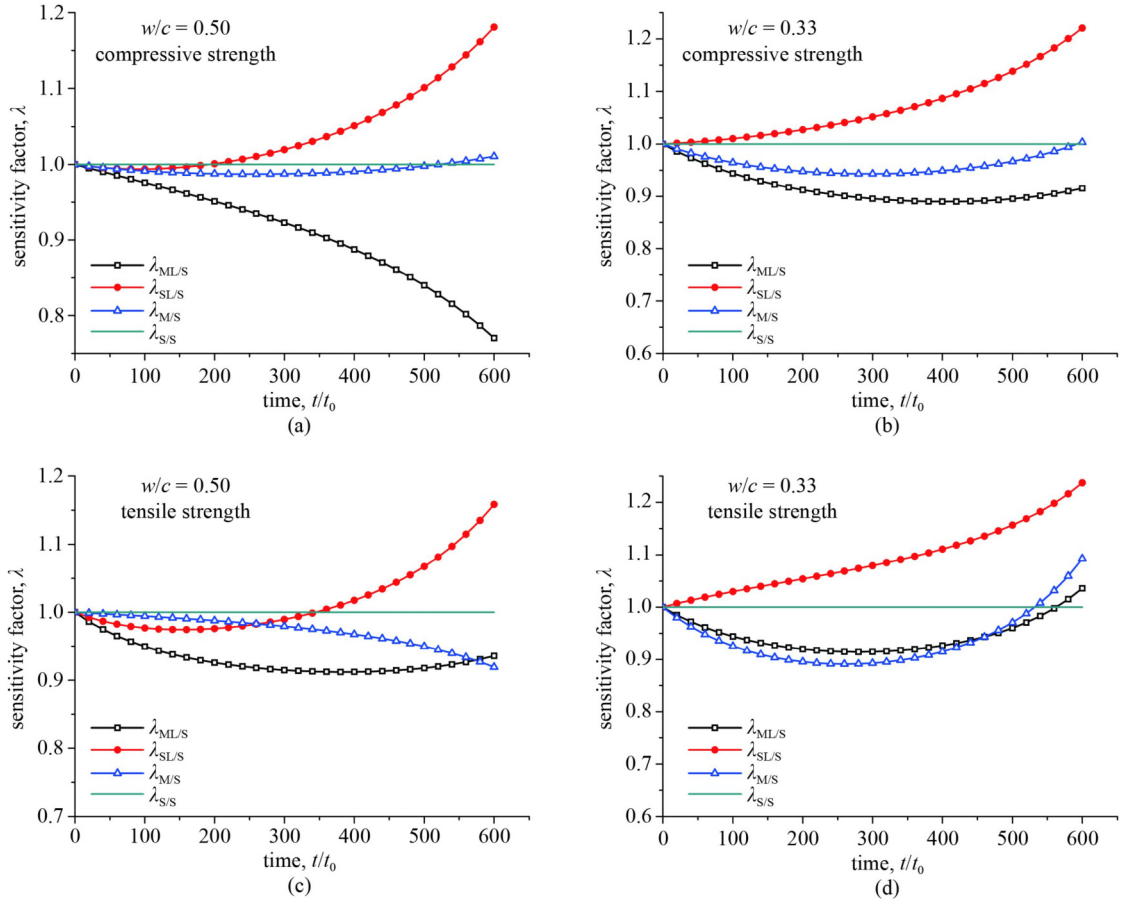

Fig. 6 Sensitivity analysis of ions in sulfate solution to the concrete strength. (a) w/c = 0.50, sensitivity analysis of compressive strength; (b) w/c = 0.33, sensitivity analysis of compressive strength; (c) w/c = 0.50, sensitivity analysis of tensile strength; (d) w/c = 0.33, sensitivity analysis of tensile strength.

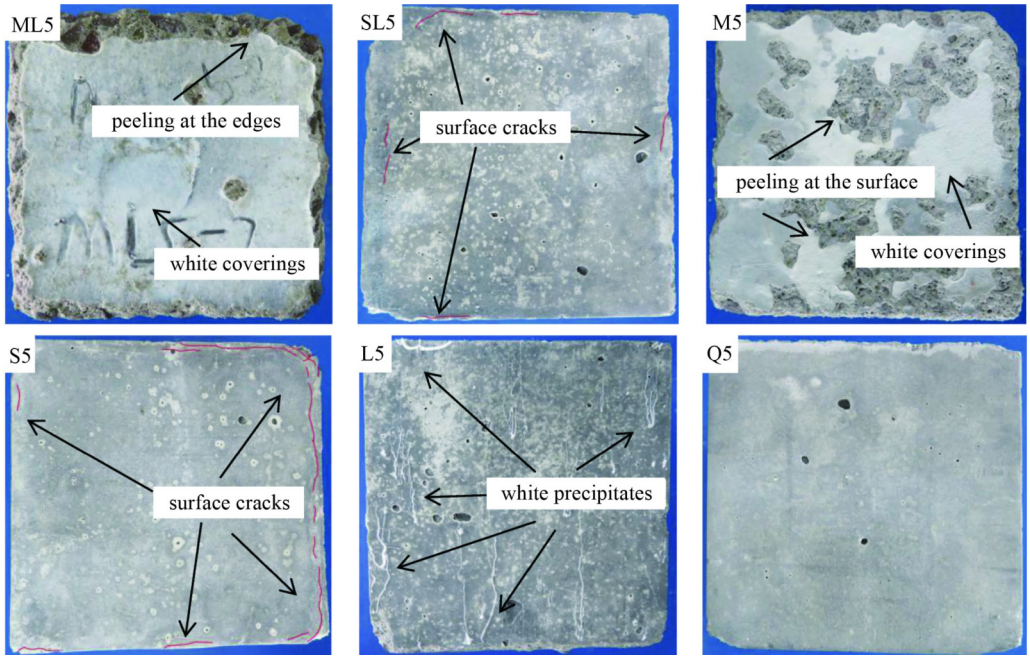

Fig. 7 Snapshots of the concrete surface in different corrosion solutions (w/c = 0.50).

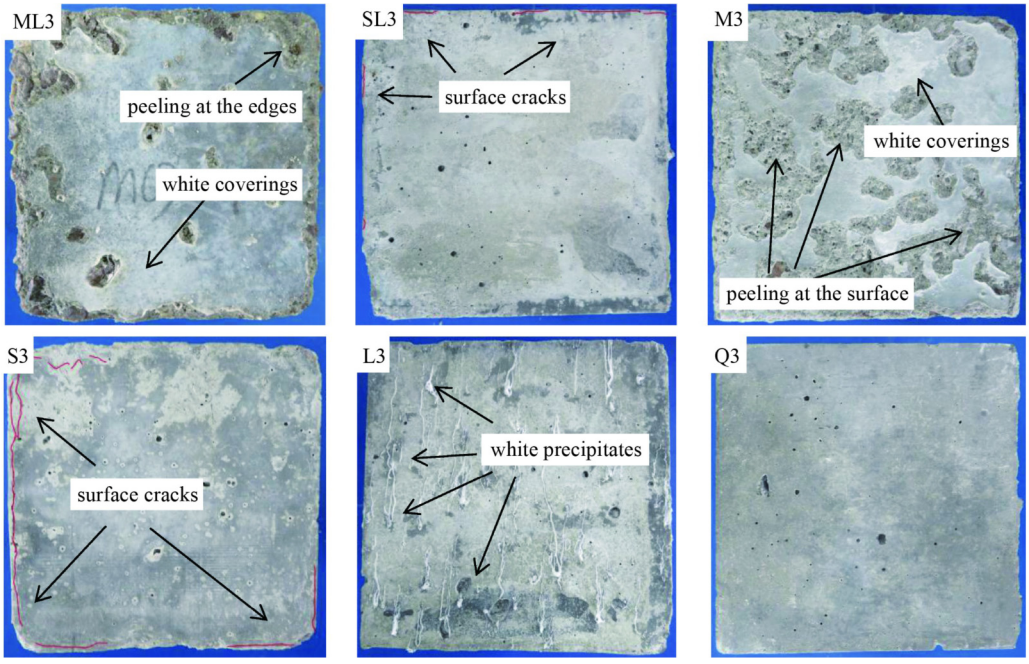

Fig. 8 Images of concrete surfaces subjected to different corrosive solutions (w/c = 0.33).

solutions, a white substance is gradually formed on the surface of specimens, but the composition of this substance is different in the two specimens. On the surface of ML5 and ML3 specimens, there is a thick white covering, and it has a certain viscosity and hygroscopicity, as shown in Fig. 9(a). On the other hand, a thin layer of white material is formed on the upper surface of the M5 and M3 specimens after drying. Through XRD detection, it is found that the white substances on the surface of ML5 and ML3 specimens contain gypsum, hydrowollastonite, sodium chloride, and magnesium hydroxide, while those on the surface of M5 and M3 specimens contain gypsum, calcium carbonate, and magnesium hydroxide.

Comparing the concrete specimens in the SL and S solutions, it can be seen that there are more cracks on the surface edges of the S5 and S3 specimens, while only few cracks are formed on the surfaces of SL5 and SL3. This is different from the observation in the magnesium sulfate solution, where the chloride ion weakens the corrosion effect of sulfate ion.

The concrete specimen immersed in just sodium chloride solution and clear water does not show any change in appearance such as edge cracks, peeling, or roughness due to corrosion. Although no corrosion damage is found on the surface of specimen immersed in only sodium chloride solution, a white substance gradually precipitates on the concrete surface after being soaked in a 10% (high concentration) sodium chloride solution for 6 months, see Fig. 9(b) for details. The smaller the water-cement ratio, the greater the amount of precipitation. The XRD analysis of this white substance shows that it mainly contains calcium carbonate with a small amount of hydrocalumite.

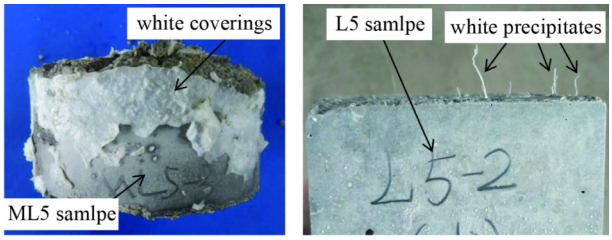

Fig. 9 White matter on concrete subjected to two corrosive solutions: (a) ML5; (b) L5.

4 Microscopic inspection and analysis of concrete corrosion products in corrosion solution

4.1 XRD test of concrete corrosion products in different corrosion solutions

The composition of the cement paste specimen after 12 months of soaking in different solutions was analyzed using XRD, and the results are shown in Fig. 10. The main corrosion products in the ML solution are ettringite, gypsum, Friedel's salt, and magnesium hydroxide. In contrast, the main corrosion products in the SL solution are ettringite and Friedel's salt. The diffraction peak intensity of the gypsum product is low, and unreacted calcium hydroxide still exists. It may be noted that the chloride ions play different roles in the corrosion process of concrete immersed in ML and SL solutions. In ML solution, the presence of chloride ions accelerates the corrosion of concrete by sulfate ions to a certain extent.

In M solution, the main corrosion products of the conc-

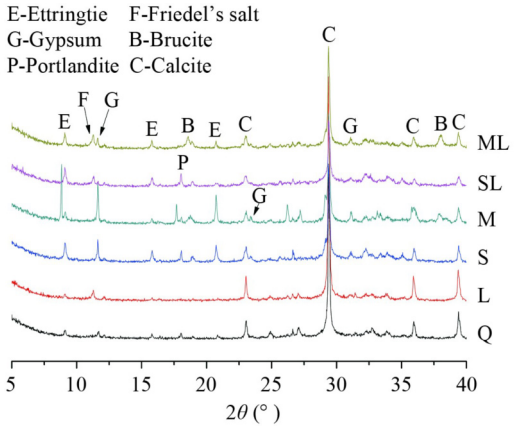

Fig. 10 XRD patterns of cement paste in different corrosive solutions.

rete material after one year of corrosion are ettringite and gypsum, and the diffraction peak intensity is significantly higher. Further, the presence of magnesium hydroxide is also detected. Compared with M solution, the corrosion products in S solution are mainly two expansive substances: ettringite and gypsum, and the diffraction peak intensity of these two substances is lower than that of the products in M solution. The main product in the L solution is Friedel's salt, while the diffraction intensity of ettringite and gypsum is low. There is a small amount of ettringite and gypsum in the hydration products in the Q solution.

The variations in the composition and quantity of the corrosion products of the specimens in the same immersion solution at different corrosion times are shown in Fig. 11. In general, as the corrosion time increases, the amount of corrosion products, such as ettringite, gypsum, shows an increasing trend, while the $Ca(OH)_2$ involved in the reaction gradually decreases. In M solution, the amount of reaction products such as ettringite and gypsum increases with increase in corrosion time. In the ML and M solutions, as the corrosion time increases, the amount of insoluble substance $Mg(OH)_2$ increases, while in the L solution, the amount of Friedel's salt increases. In SL and Q solutions, the types and quantities of the chemical reaction products remain basically unchanged with the increase in immersion time. In fact, ettringite expansion is suppressed, where OH^- ions have been replaced by Cl^- ions. This is because that an alkaline environment is necessary for the swelling of ettringite.

4.2 SEM test and energy spectrum analysis of concrete corrosion products in different corrosion solutions

After concrete specimens were soaked in the corrosion solutions for 12 months, some small fragments were taken from the specimens after the strength test, and the microscopic morphology and elemental composition of the corrosion products were investigated using SEM and energy spectrum analysis, respectively. The micro morphology and energy spectra of the concrete corrosion products in the six different solutions are shown in Figs. 12 and 13, respectively. The elemental composition of the corrosion products numbered ①–⑥ in Fig. 12 are indicated by the corresponding numbers in Fig. 13. The main substance of serial number ① is gypsum, the main component of serial numbers ② and ③ is ettringite, the component of serial number ④ is C−S−H gel, the component of serial number ⑤ should be Friedel's salt, and the serial number ⑥ is calcium hydroxide.

As shown in Fig. 12(a), a large amount of corrosion products containing gypsum and ettringite (represented by the symbol AFt) is observed in the concrete materials in ML solution. In contrast, there are fewer corrosion products inside the concrete in SL solution, and a small amount of ettringite is found, as shown in Fig. 12(b). It can be seen from Fig. 12(c) that the corrosion products in M solution are similar to that in ML solution, and a large amount of gypsum and ettringite is also found in the concrete materials. For the concrete material immersed in S solution, ettringite is found in the corrosion products, and its quantity is higher at the interface around the aggregate, as shown in Fig. 12(d). For the concrete in the L solution, more C−S−H gel is produced, which contains some flaky Friedel's salt, as shown in Fig. 12(e). For the concrete in the Q solution, Ca $(OH)_2$ is observed, and a small amount of ettringite exists in the C−S−H gel, as shown in Fig. 12(f).

From XRD and SEM analyses, it is known that the main corrosion products in the composite solution of magnesium sulfate and sodium chloride are ettringite, gypsum, Friedel's salt, and magnesium hydroxide. In contrast, the main corrosion products in the composite solution of sodium sulfate and sodium chloride are only ettringite and Friedel's salt.

In the composite solution of sodium sulfate and sodium chloride, chloride ions have an inhibitory effect on the corrosion of sulfate ions. The reason is that the chloride ion in the solution diffuses faster than the sulfate ion [14]. Therefore, chloride ions will enter the concrete material before sulfate ions and chemically react with hydration products to form Friedel's salt, which then fills up the internal pores and delays the penetration rate of sulfate ions into the material.

However, in the composite solution of magnesium sulfate and sodium chloride, once the magnesium ions in the corrosive solution enter the concrete pores, the $Ca(OH)_2$ in the internal solution will be reduced. The chemical reaction will produce gypsum and magnesium hydroxide with very little solubility. Furthermore, the pH value in the pore solution will decrease, which may cause the C−S−H gel to decalcify and convert it into M−S−H. And M−S−H has no adhesiveness, which will cause the concrete structure to become loose and the strength will be greatly reduced. As the corrosion time increases,

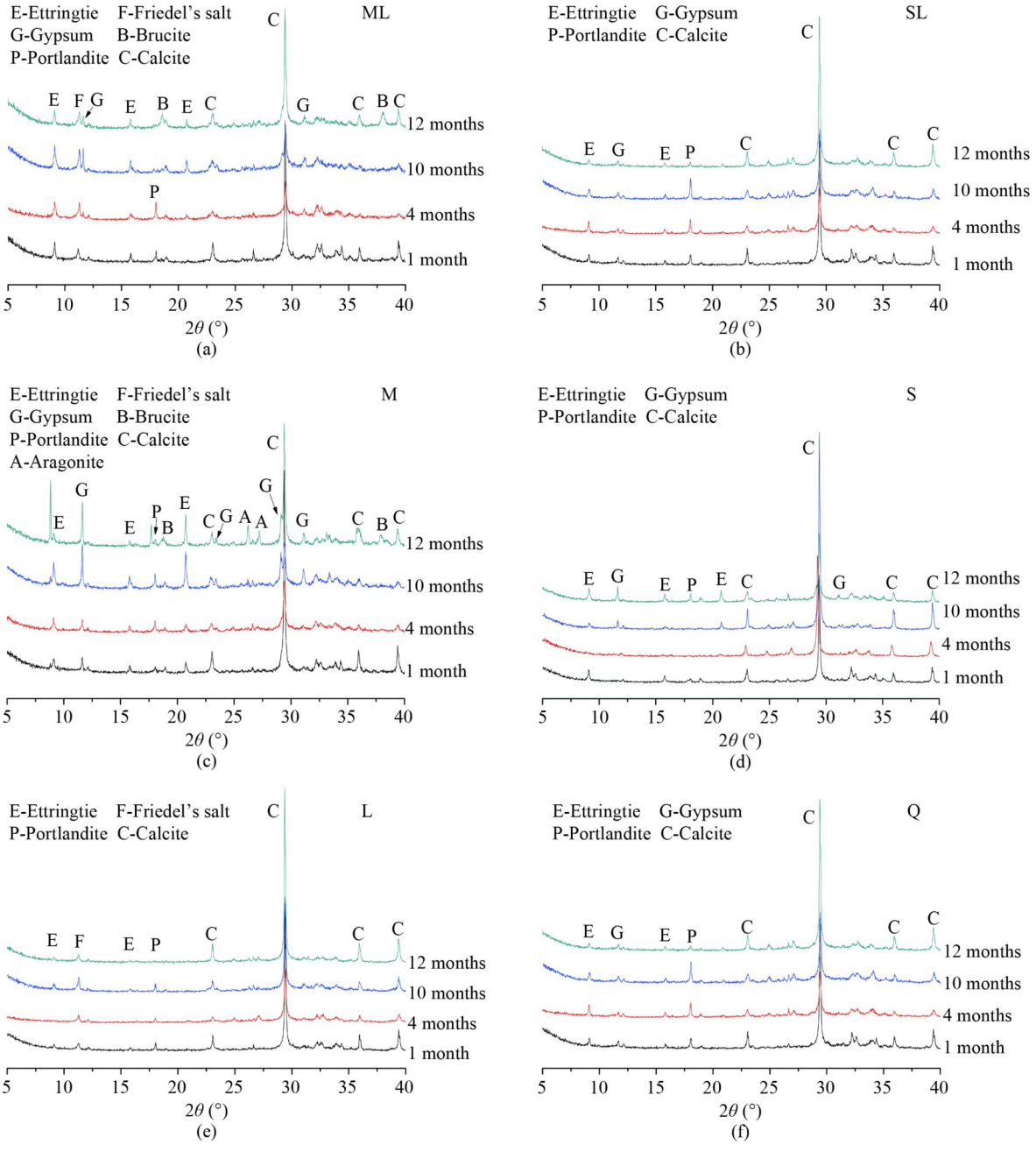

Fig. 11 XRD patterns of cement paste at different corrosion times: (a) ML; (b) SL; (c) M; (d) S; (e) L; (f) Q.

sulfate ions and chloride ions will further attack the material itself. Therefore, the intervention of magnesium ions will transform the inhibitory effect on corrosion of chloride ions on sulfate ion into a promoting effect.

5 Conclusions

The macroscopic physical and mechanical properties, microscopic morphology, and chemical composition of concrete materials with different water-cement ratios in different corrosive solutions were studied. The sensitivity of each ion to continued hydration was analyzed, and the impact of the interaction of Cl^- and Mg^{2+} on the corrosion damage caused by SO_4^{2-} was examined. The main results of the study are summarized as follows.

1) The variation in the strength of concrete in multi-salt solution with corrosion time revealed two distinct aspects. On the one hand, the unhydrated cement products continued to undergo hydration reaction to form new C−S−H gels, which promoted an increase in concrete strength. On the other hand, the ions in the solution invaded the internal pores of the concrete and reacted with the pore solution to form corrosion products, which in some promoted and in other cases inhibited the growth of concrete strength.

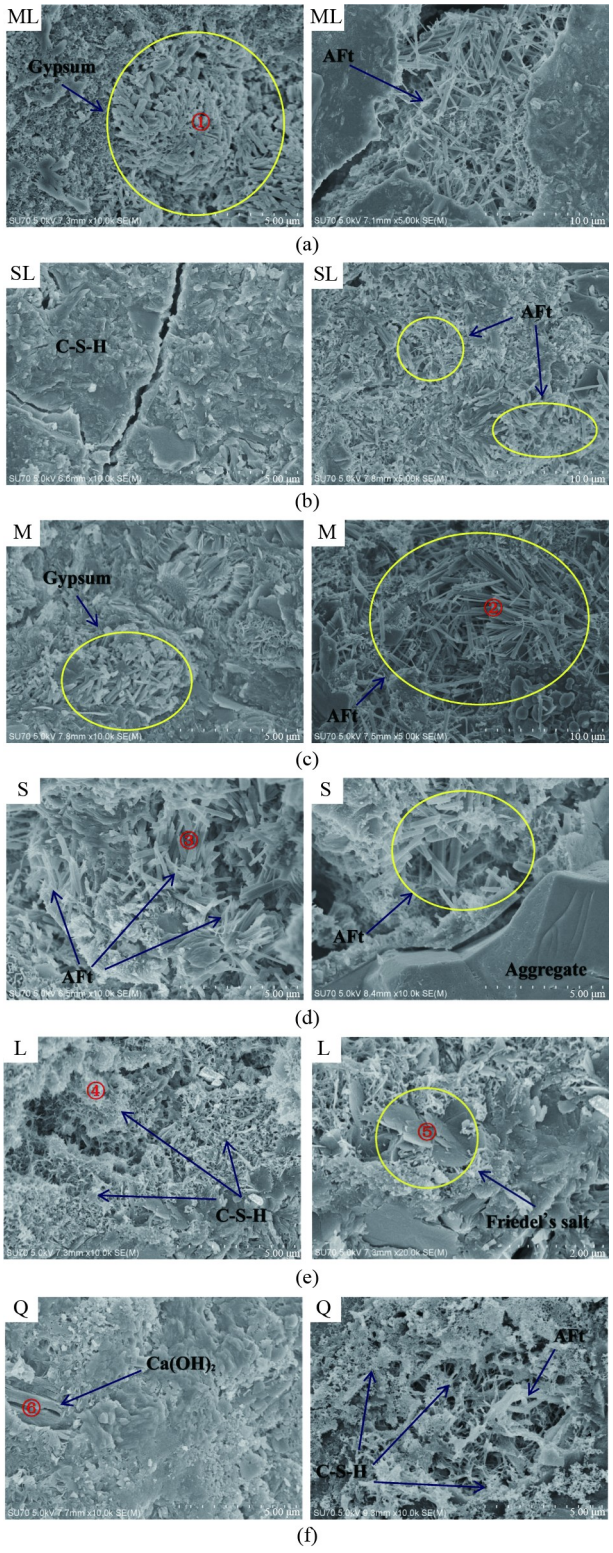

Fig. 12 SEM images of concrete fragments in different solutions: (a) ML; (b) SL; (c) M; (d) S; (e) L; (f) Q.

2) By introducing the sensitivity factor, the effect of various corrosive ions to the deterioration of concrete strength was studied. It was observed that the influence of each ion on the tensile and compressive strength of concrete exhibited a trend of strengthening first and then weakening. However, it may be noted that the Cl^- in a solution with sodium chloride was effect to the compressive strength of concrete, but the sensitivity of the tensile strength was very small, i.e., the chloride ion had little or no effect on the tensile strength.

3) The sensitivity of the addition of a single kind of Cl^- to SO_4^{2-} in the sulfate solution was examined quantitatively. The results indicated that Cl^- slowed down the corrosion of concrete caused by SO_4^{2-} by approximately 20%. However, the addition of Mg^{2+} or Mg^{2+} and Cl^- promoted it by 10%–20%. Further, in general, Mg^{2+} and Cl^- had a stronger strengthening effect than just Mg^{2+}.

4) XRD and SEM were used to determine the corrosion product composition of concrete materials, and the microscopic damage mechanism of concrete samples was analyzed. Based on a comprehensive analysis of macro-physical, mechanical properties and micro-corrosion mechanism, it was inferred that the degree of corrosion damage to concrete by different salt solutions followed this order: Solution of magnesium sulfate and sodium chloride > Solution of magnesium sulfate > Solution of sodium sulfate > Solution of sodium sulfate and sodium chloride > Solution of sodium chloride.

This work is aimed at filling a gap in existing research, which fails to quantitatively study the effect of the ion interaction in multi-salt solutions on the strength of concrete. The sensitivity analysis method based on concrete strength is used to consider the quantitative analysis of the sensitivity of concrete strength to the interaction of various ions in the multi-salt solution. In the future work, this analysis method can be helpful to establish the corrosion damage model of concrete structures under multi-salt corrosion, and it is also of great significance to consider accurate prediction of the entire service life of concrete materials from initial to complete deterioration.

Acknowledgments The authors would like to acknowledge the financial support by the National Natural Science Foundation of China (Grant Nos. 11832013 and 11772164), the project of Key Laboratory of Impact and Safety Engineering (Ningbo University), Ministry of Education (No. cj202004), and the Natural Science Foundation Project of Ningbo (No. 202003N4319), the Research and Innovation Team Funded Project of Zhejiang Business Technology Institute (No. KYTD202106), the Marine Biotechnology and Marine Engineering Discipline Group in Ningbo University, and K.C. Wong Magna Fund in Ningbo University. The authors thank Professor Weidong Zhou of Zhenjiang Zhuanbo Detection Technology Co., Ltd. for his help in the SEM detection.

Notations

Q: clear water solution
L: 10% sodium chloride solution
S: 5% sodium sulfate solution

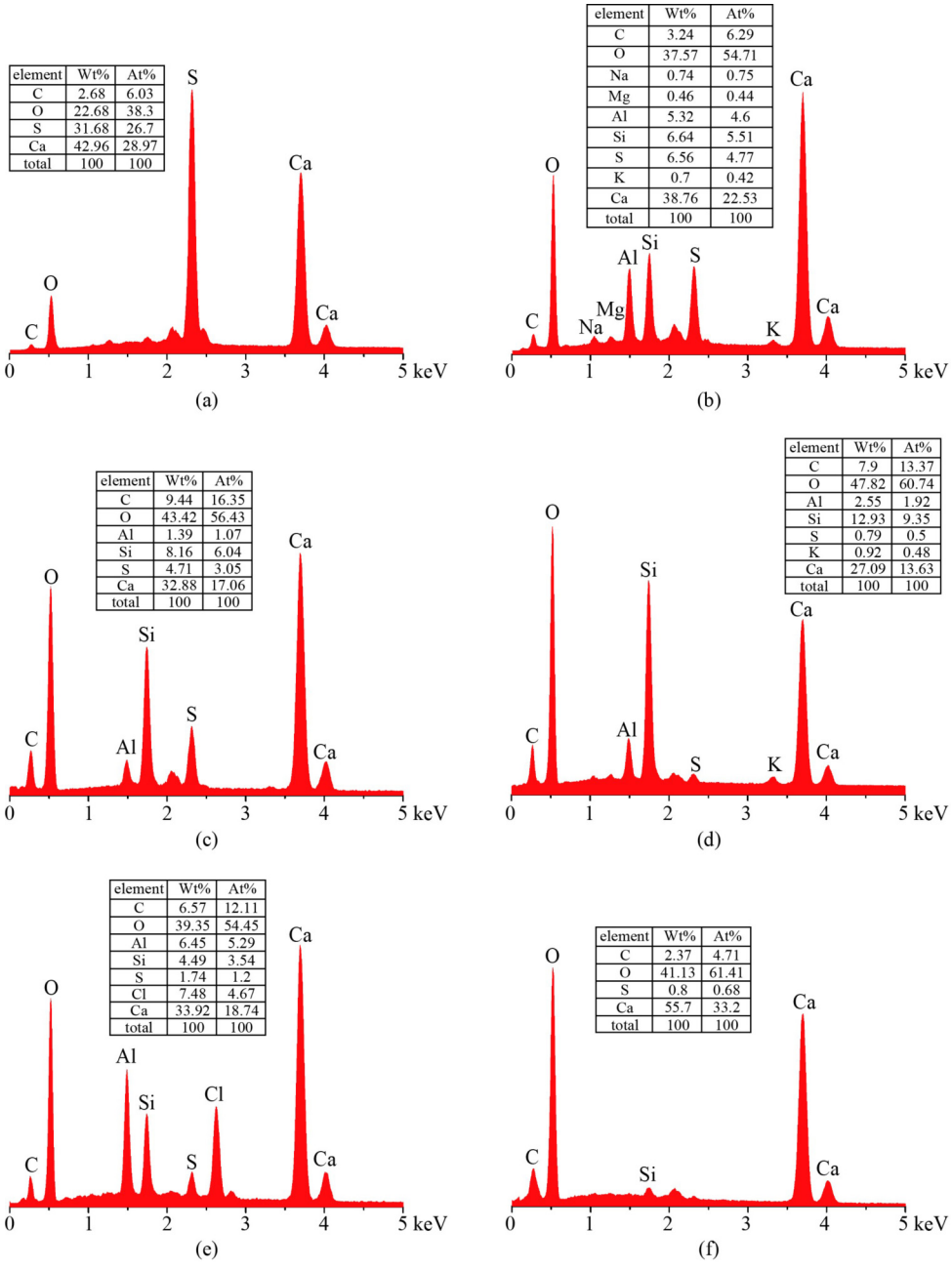

Fig. 13 Energy spectra of corrosion products. (a) ①; (b) ②; (c) ③; (d) ④; (e) ⑤; (f) ⑥ in Fig. 12.

M: 5% magnesium sulfate solution

SL: mixed solution of 5% sodium sulfate and 10% sodium chlorid

ML: mixed solution of 5% magnesium sulfate and 10% sodium chloride

Q5, Q3: concrete specimens with *w*/*c* = 0.50 or 0.33 in clear water solution

L5, L3: concrete specimens with *w*/*c* = 0.50 or 0.33 in sodium chloride solution

S5, S3: concrete specimens with *w*/*c* = 0.50 or 0.33 in sodium sulfate solution

M5, M3: concrete specimens with *w*/*c* = 0.50 or 0.33 in magnesium sulfate solution

SL5, SL3: concrete specimens with *w*/*c* = 0.50 or 0.33 in mixed solution of sodium sulfate and sodium chloride

ML5, ML3: concrete specimens with *w*/*c* = 0.50 or 0.33 in mixed solution of magnesium sulfate and sodium chloride

q5, q3: concrete strength with *w*/*c* = 0.50 or 0.33 in clear water solution

l5, l3: concrete strength with *w*/*c* = 0.50 or 0.33 in sodium chloride solution

s5, s3: concrete strength with *w*/*c* = 0.50 or 0.33 in sodium sulfate solution

m5, m3: concrete strength with *w*/*c* = 0.50 or 0.33 in magnesium sulfate solution

sl5, sl3: concrete strength with *w*/*c* = 0.50 or 0.33 in mixed

solution of sodium sulfate and sodium chloride

ml5, ml3: concrete strength with w/c = 0.50 or 0.33 in mixed solution of magnesium sulfate and sodium chloride

References

1. Poupard O, L'Hostis V, Catinaud S, Petre-Lazar I. Corrosion damage diagnosis of a reinforced concrete beam after 40 years natural exposure in marine environment. Cement and Concrete Research, 2006, 36(3): 504−520
2. Da B, Yu H F, Ma H Y, Tan Y S, Mi R J, Dou X M. Chloride diffusion study of coral concrete in a marine environment. Construction & Building Materials, 2016, 123: 47−58
3. Cang S, Yang Y Z, Chen J K. Damage layer evolution of a breakwater under seawater attack: testing and modeling. Acta Mechanica Solida Sinica, 2020, 33(1): 1−13
4. Lei L, Wang Q, Xu S, Wang N, Zheng X. Fabrication of superhydrophobic concrete used in marine environment with anti-corrosion and stable mechanical properties. Construction & Building Materials, 2020, 251: 118946
5. Wu Z Y, Yu H F, Ma H Y, Zhang J H, Da B, Zhu H W. Rebar corrosion in coral aggregate concrete: Determination of chloride threshold by LPR. Corrosion Science, 2020, 163: 108238
6. Wang X Y. Impacts of climate change on optimal mixture design of blended concrete considering carbonation and chloride ingress. Frontiers of Structural and Civil Engineering, 2020, 14(2): 473−486
7. Qiao C, Suraneni P, Weiss J. Damage in cement pastes exposed to NaCl solutions. Construction & Building Materials, 2018, 171: 120−127
8. Xu H, Chen J K. Coupling effect of corrosion damage on chloride ions diffusion in cement based materials. Construction & Building Materials, 2020, 243: 118225
9. Jiang L, Niu D T. Study of deterioration of concrete exposed to different types of sulfate solutions under drying−wetting cycles. Construction & Building Materials, 2016, 117: 88−98
10. Zhang M H, Chen J K, Lv Y F, Wang D J, Ye J. Study on the expansion of concrete under attack of sulfate and sulfate–chloride ions. Construction & Building Materials, 2013, 39: 26−32
11. Sotiriadis K, Nikolopoulou E, Tsivilis S, Pavlou A, Chaniotakis E, Swamy R N. The effect of chlorides on the thaumasite form of sulfate attack of limestone cement concrete containing mineral admixtures at low temperature. Construction & Building Materials, 2013, 43: 156−164
12. Chen Y, Gao J, Tang L, Li X. Resistance of concrete against combined attack of chloride and sulfate under drying–wetting cycles. Construction & Building Materials, 2016, 106: 650−658
13. Yin R R, Zhang C C, Wu Q, Li B C, Xie H. Damage on lining concrete in highway tunnels under combined sulfate and chloride attack. Frontiers of Structural and Civil Engineering, 2018, 12(3): 331−340
14. Maes M, de Belie N. Resistance of concrete and mortar against combined attack of chloride and sodium sulphate. Cement and Concrete Composites, 2014, 53: 59−72
15. Zuo X B, Sun W, Yu C. Numerical investigation on expansive volume strain in concrete subjected to sulfate attack. Construction & Building Materials, 2012, 36: 404−410
16. Mao L X, Hu Z, Xia J, Feng G L, Azim I, Yang J, Liu Q F. Multi-phase modelling of electrochemical rehabilitation for ASR and chloride affected concrete composites. Composite Structures, 2019, 207: 176−189
17. Jiang W Q, Shen X H, Hong S X, Wu Z Y, Liu Q F. Binding capacity and diffusivity of concrete subjected to freeze-thaw and chloride attack: a numerical study. Ocean Engineering, 2019, 186: 106093
18. Li L J, Liu Q F, Tang L P, Hu Z, Wen Y, Zhang P. Chloride penetration in freeze-thaw induced cracking concrete: A numerical study. Construction & Building Materials, 2021, 302: 124291
19. Liu Q F, Iqbal M F, Yang J, Lu X Y, Zhang P, Rauf M. Prediction of chloride diffusivity in concrete using artificial neural network: Modelling and performance evaluation. Construction & Building Materials, 2021, 268: 121082
20. Ikumi T, Segura I. Numerical assessment of external sulfate attack in concrete structures: A review. Cement and Concrete Research, 2019, 121: 91−105
21. Zhang C L, Chen W K, Mu S, Šavija B, Liu Q F. Numerical investigation of external sulfate attack and its effect on chloride binding and diffusion in concrete. Construction & Building Materials, 2021, 285: 122806
22. Shen X H, Liu Q F, Hu Z, Jiang W Q, Lin X S, Hou D H, Hao P. Combine ingress of chloride and carbonation in marine-exposed concrete under unsaturated environment: a numerical study. Ocean Engineering, 2019, 189: 106350
23. de Weerdt K, Orsáková D, Geiker M R. The impact of sulphate and magnesium on chloride binding in Portland cement paste. Cement and Concrete Research, 2014, 65: 30−40
24. Xie N, Dang Y, Shi X. New insights into how $MgCl_2$ deteriorates Portland cement concrete. Cement and Concrete Research, 2019, 120: 244−255
25. Damrongwiriyanupap N, Li L Y, Xi Y P. Coupled diffusion of chloride and other ions in saturated concrete. Frontiers of Structural and Civil Engineering, 2011, 5(3): 267−277
26. Hekal E E, Kishar E, Mostafa H. Magnesium sulfate attack on hardened blended cement pastes under different circumstances. Cement and Concrete Research, 2002, 32(9): 1421−1427
27. de Weerdt K, Justnes H. The effect of sea water on the phase assemblage of hydrated cement paste. Cement and Concrete Composites, 2015, 55: 215−222
28. Maes M, Mittermayr F, de Belie N. The influence of sodium and magnesium sulphate on the penetration of chlorides in mortar. Materials and Structures, 2017, 50(2): 1−14
29. Al-Amoudi O S B, Maslehuddin M, Abdul-Al Y A B. Role of chloride ions on expansion and strength reduction in plain and blended cements in sulfate environments. Construction & Building Materials, 1995, 9(1): 25−33
30. Chiker T, Aggoun S, Houari H, Siddique R. Sodium sulfate and alternative combined sulfate/chloride action on ordinary and self-consolidating PLC-based concretes. Construction & Building Materials, 2016, 106: 342−348
31. Chen F, Gao J, Qi B, Shen D, Li L. Degradation progress of concrete subject to combined sulfate-chloride attack under

drying−wetting cycles and flexural loading. Construction & Building Materials, 2017, 151: 164−171

32. Yu H F, Tan Y S, Yang L M. Microstructural evolution of concrete under the attack of chemical, salt crystallization, and bending stress. Journal of Materials in Civil Engineering, 2017, 29(7): 04017041
33. Maes M, de Belie N. Influence of chlorides on magnesium sulphate attack for mortars with Portland cement and slag based binders. Construction & Building Materials, 2017, 155: 630−642
34. Geng J, Easterbrook D, Li L Y, Mo L W. The stability of bound chlorides in cement paste with sulfate attack. Cement and Concrete Research, 2015, 68: 211−222
35. Sotiriadis K, Nikolopoulou E, Tsivilis S. Sulfate resistance of limestone cement concrete exposed to combined chloride and sulfate environment at low temperature. Cement and Concrete Composites, 2012, 34(8): 903−910
36. Brown P W, Badger S. The distributions of bound sulfates and chlorides in concrete subjected to mixed NaCl, $MgSO_4$, Na_2SO_4 attack. Cement and Concrete Research, 2000, 30(10): 1535−1542